Suplemento de la Revista Mexicana de Física **3** 0308033 (2022) 1–7

Quarkoniumlike mesons in the diabatic approach

R. Bruschini

Unidad Teórica, Instituto de Física Corpuscular
(Universidad de Valencia–CSIC), E-46980 Paterna (Valencia), Spain

Received 27 October 2021; accepted 18 November 2021

The Born-Oppenheimer approximation provides a description of heavy-quark mesons firmly based on quenched Lattice QCD. The diabatic framework extends this description through the incorporation of unquenched Lattice QCD data on string breaking. This allows for a unified description of conventional quarkonium, made of $Q\bar{Q}$, and unconventional quarkoniumlike mesons, containing meson-meson components as well. A successful description of the charmoniumlike and bottomoniumlike spectra comes out.

Keywords: Quark; meson; potential.

DOI: https://doi.org/10.31349/SuplRevMexFis.3.0308033

1. Introduction

A new era in heavy-quark meson spectroscopy begun with the discovery of the $X(3872)$ [1]. In fact, this was among the first states whose mass and decay properties clearly defied expectations from potential quark models, which had been so successful until then [2–4]. Soon enough, the $X(3872)$ was joined by many other resonances (e.g.: $\psi(4260)$, $\psi(4360)$, $X(3915)$, see [5]) which escape the quarkonium description ($Q\bar{Q}$, with Q a heavy quark), thus forming the spectrum of so-called XYZ states. The understanding of these unconventional mesons, possibly with a solid theoretical basis on quantum chromodynamics (QCD), is presently one of the greatest challenges in hadronic physics.

As a matter of fact, the masses of the unconventional states are generally located close below or above the lowest open-flavor meson-meson threshold coupling to them, which suggests that any theoretical description of them should include open-flavor meson-meson components. Potential quark models (see, for example, [2, 3, 6, 7]) partly take this into account through meson loops. In some of these models [2, 3], the coupling between the valence $Q\bar{Q}$ states and the meson-meson continuum is derived from the $Q\bar{Q}$ binding potentials, while others [6, 7] use quark pair creations models such as $^3P_0$. Anyhow, these loop contributions do not seem effective at describing the rich spectrum of unconventional states. In alternative, other phenomenological descriptions including meson-meson components, like, for example, in the form of meson molecules, tetraquarks, and hadroquarkonium (see [8–11] and references therein), have been attempted. It must be noted though that all these models, including the aforementioned quark models with meson loops, lack a direct connection with QCD.

An *ab initio* description of heavy-quark mesons from Lattice QCD has been developed using a Born-Oppenheimer (BO) approximation [12, 13], which can also be connected with an effective field theoretical description (see, for instance, [14]). The single-channel BO approximation is based on the heavy-quark mass being much larger than the QCD energy scale $\Lambda_{\rm QCD}$, so that heavy-quark meson states correspond to the solutions of a Schrödinger equation for $Q\bar{Q}$ with effective potentials derived from Lattice QCD. These potentials correspond to the energy of stationary states of light fields (light quark flavors and gluons) with static color sources. Conventional quarkonium states thus correspond to the solutions of the ground state potential, calculated in quenched Lattice QCD (*i.e.*, neglecting sea quarks), which has a Cornell-like shape familiar from quark models [15]. Quarkonium hybrids (a quark-antiquark pair in presence of an excited gluon field, sometimes referred to as a $Q\bar{Q}g$ state with g a constituent gluon) are the solutions of the excited-state potentials calculated in quenched Lattice QCD [12]. However, the single-channel BO approximation is not as effective when meson-meson components start to play some role. In fact, unquenched (including sea quarks) Lattice QCD calculations of the static energy levels [16, 17] show that as the $Q\bar{Q}$ potential approaches the mass of a meson-meson threshold, a mixing between the two configurations takes place. This mixing, due to string breaking from creation of sea quark pairs, breaks the single-channel BO approximation. Therefore, the single-channel BO approximation is valid only for energies far below any meson-meson threshold, which limits considerably its utility for the description of the unconventional states.

In this talk we go beyond the single-channel BO approximation by adapting the diabatic approach, first developed in molecular physics (see, for example, [18]), to the description of quarkonium(-like) mesons in terms of $Q\bar{Q}$ and open-flavor meson-meson components. In this way we establish a coherent and unified theoretical framework, firmly based on QCD, for the description of both conventional and unconventional states [19–21]. These contents are structured as follows. First, in Sec. 2, we revisit the single-channel BO approximation in its application to quarkoniumlike mesons. Then, in Sec. 3, we introduce the diabatic formalism and connect it to lattice data. In Sec. 4, we recollect the results of a diabatic study of the charmoniumlike and bottomoniumlike spectra. Finally, in Sec. 5, we summarize our conclusions.

2. Born-Oppenheimer approximation

The BO approximation was originally derived for the description of molecules [22], but more recently it has been also applied to the description of heavy-quark meson systems from Lattice QCD [12,13]. As the heavy quarks have a mass much larger than $\Lambda_{\rm QCD}$, on the contrary of the light fields (this is, gluons and light quark flavors), it is assumed that the Hamiltonian of the heavy-quark system can be separated as

$$H = K_{Q\bar{Q}} + H^{\rm lf}_{Q\bar{Q}}, \tag{1}$$

where $K_{Q\bar{Q}}$ is the heavy quark-antiquark ($Q\bar{Q}$) kinetic energy operator and the residual Hamiltonian $H^{\rm lf}_{Q\bar{Q}}$ includes the light-field Hamiltonian and the $Q\bar{Q}$–light-field interaction, but contains no dependence on the $Q\bar{Q}$ momentum $\boldsymbol{p}$. A quarkoniumlike meson state $|\psi\rangle$, containing information on the $Q\bar{Q}$ as well as the light fields, then corresponds to a solution of

$$H\,|\psi\rangle = E\,|\psi\rangle\,, \tag{2}$$

where E is its energy.

The first step in the construction of the BO approximation consists in integrating the light fields for static $Q\bar{Q}$, which corresponds to ignoring the kinetic energy term $K_{Q\bar{Q}}$. This static limit is justified as long as the time scale for the evolution of the $Q\bar{Q}$ (proportional to their reduced mass) is so much larger than so that of the light fields, that the dynamics of the latter can be solved as if the former were not moving at all. In this limit the quark-antiquark relative position $\boldsymbol{r}$ is fixed, and thus ceases to be a dynamical variable. Consequently, $H^{\rm lf}_{Q\bar{Q}}$ depends only parametrically on $\boldsymbol{r}$, and can be therefore relabeled as $H^{\rm lf}_{\rm static}(\boldsymbol{r})$. Integrating the light fields in the static limit then corresponds to solving, for any fixed value of $\boldsymbol{r}$, the eigenvalue problem

$$(H^{\rm lf}_{\rm static}(\boldsymbol{r}) - V_i(\boldsymbol{r}))\,|\zeta_i(\boldsymbol{r})\rangle = 0, \tag{3}$$

where $|\zeta_i(\boldsymbol{r})\rangle$ is the light-field eigenstate, $V_i(\boldsymbol{r})$ its eigenvalue, and i some quantum numbers labeling the eigenstate. Notice that, altogether, the eigenstates $\{|\zeta_i(\boldsymbol{r})\rangle\}_i$ form an orthonormal basis set for the Hilbert space of light-field configurations

$$\langle\zeta_i(\boldsymbol{r})|\zeta_j(\boldsymbol{r})\rangle = \delta_{ij}, \tag{4}$$

for any $\boldsymbol{r}$. Then an eigenvalue $V_i(\boldsymbol{r})$ corresponds to the static energy of a stationary light-field configuration $|\zeta_i(\boldsymbol{r})\rangle$, with a $Q\bar{Q}$ pair fixed at relative position $\boldsymbol{r}$, which can be calculated *ab initio* in Lattice QCD.

The ground state of the light fields in quenched (neglecting sea quarks) Lattice QCD is associated with a quarkonium $Q\bar{Q}$ configuration [15]. Its energy follows the behavior of a Cornell (funnel) potential, as pictured in Fig. 1. However, unquenched (including sea quarks) Lattice QCD calculations have shown that this correspondence is valid only for small $Q\bar{Q}$ distances [16, 17]. In fact, when increasing the $Q\bar{Q}$ distance $r = |\boldsymbol{r}|$, a significant mixing between the $Q\bar{Q}$ configuration and meson-meson ones takes place in the ground state

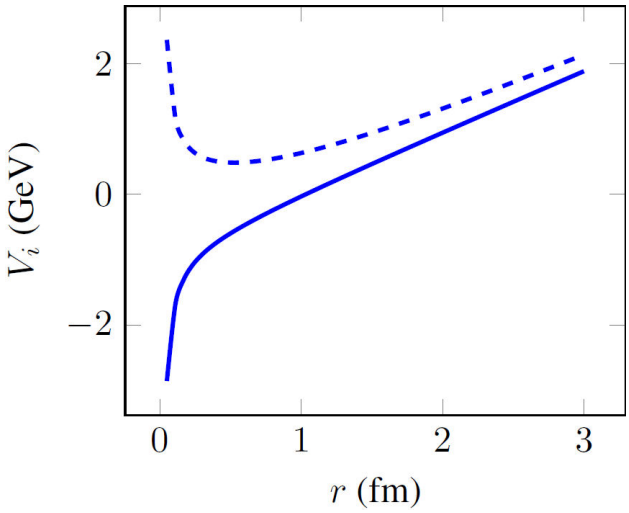

FIGURE 1. Radial dependence of the ground (solid line) and first excited (dashed line) quenched static energies, $\widetilde{V}_i(r)$.

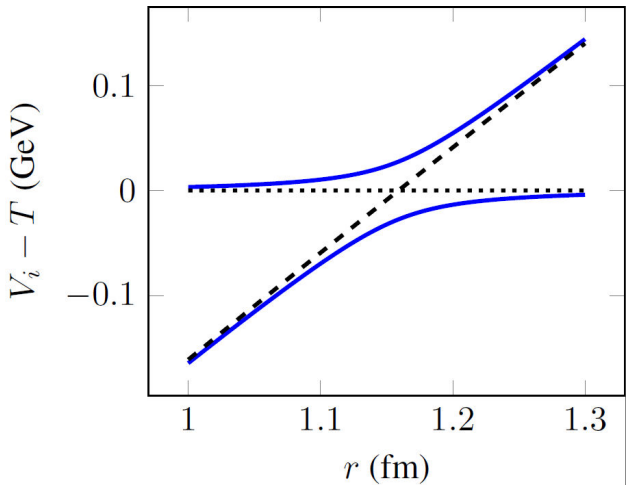

FIGURE 2. Radial dependence of the ground and first excited unquenched static energies, $V_i(r)$, normalized with respect to the threshold mass T, near the avoided crossing (solid lines). The quenched ground state energy (dashed line) and the meson-meson threshold (dotted line) are also drawn for comparison.

because of string breaking. If for example we consider $Q\bar{Q}$ in presence of only one threshold, the unquenched ground state energy changes progressively from the one of a $Q\bar{Q}$ configuration to that of the meson-meson one. At the same time, an excited state appears with the opposite behavior, this is, its energy changes from meson-meson to $Q\bar{Q}$ as r increases. In this manner, the ground and excited energy levels avoid the crossing of the pure $Q\bar{Q}$ energy with the meson-meson threshold (which would happen if string breaking were not present). In Fig. 2 we have pictured this situation, whereas a representation of $Q\bar{Q}$ interacting with two thresholds can be found in Ref. [16, 17].

As second step in building the BO approximation, the $Q\bar{Q}$ motion is solved by reintroducing $K_{Q\bar{Q}}$ and using the

adiabatic expansion

$$|\psi\rangle = \sum_j \int \mathrm{d}\boldsymbol{r}' \psi_j(\boldsymbol{r}') \, |\boldsymbol{r}'\rangle \, |\zeta_j(\boldsymbol{r}')\rangle \,, \tag{5}$$

where $|\boldsymbol{r}'\rangle$ is the $Q\bar{Q}$ relative position eigenstate, $\psi_j(\boldsymbol{r}')$ are the expansion coefficients, and we have omitted spin degrees of freedom, for simplicity. Notice that the light-field basis used in this expansion is calculated at the same relative position $\boldsymbol{r}'$ as the $Q\bar{Q}$, which is the most natural choice in the idealized situation where the light fields adjust immediately to the $Q\bar{Q}$ motion, hence the qualifier "adiabatic" . Because of this, the kinetic energy operator $K_{Q\bar{Q}}$ acts also on the light-field states, so deriving an equation involving the expansion coefficients requires some simple but lengthy manipulations. Eventually, Eq. (2) can be rewritten as (see, for example, [18])

$$\sum_j \Big[-\frac{\hbar^2}{2\mu_{Q\bar{Q}}} ((\boldsymbol{\nabla} + \boldsymbol{\tau}(\boldsymbol{r}))^2)_{ij} + (V_i(\boldsymbol{r}) - E)\delta_{ij} \Big] \psi_j(\boldsymbol{r}) = 0, \tag{6}$$

where $\mu_{Q\bar{Q}}$ is the reduced $Q\bar{Q}$ mass and

$$\boldsymbol{\tau}_{ij}(\boldsymbol{r}) \equiv \langle \zeta_i(\boldsymbol{r}) | \boldsymbol{\nabla} \zeta_j(\boldsymbol{r}) \rangle \,, \tag{7}$$

are the so-called *Non-Adiabatic Coupling Terms* (NACTs), which reflect the non-trivial interaction between the $Q\bar{Q}$ motion and the light-field eigenstates. Now the expansion coefficients $\psi_j(\boldsymbol{r})$ can be recognized as the components of a multichannel adiabatic wave function, governed by a Schrödinger-like equation where the static energies $V_i(\boldsymbol{r})$ act as effective potentials. However, the presence of these NACTs, mixing different channels through the kinetic energy term, complicates extraordinarily the solution of Eq. (6). That is why it is customary to neglect the NACTs,

$$\boldsymbol{\tau}_{ji}(\boldsymbol{r}) \approx 0, \tag{8}$$

so that one is left with the set of decoupled single-channel equations

$$\left[-\frac{\hbar^2}{2\mu_{Q\bar{Q}}} \nabla^2 + (V_i(\boldsymbol{r}) - E) \right] \psi_i(\boldsymbol{r}) = 0. \tag{9}$$

Equations (3), (5), (8), and (9) constitute the core of the BO approximation, in its usual single-channel realization. Regarding its usefulness, unquenched lattice calculations indicate that the NACTs are only negligible when no $Q\bar{Q}$ and meson-meson configuration mixing takes place within the light-field eigenstates (see the next section). This is a serious drawback for the application of the single-channel BO approximation to the description of heavy-quark mesons, whose masses are usually located close below, or above, the lowest open-flavor meson-meson threshold, where a significant mixing induced by string breaking may be present.

3. Diabatic approach

To overcome the limitations of the single-channel BO approximation, we make use of the *diabatic formalism*. In this framework, instead of using light field eigenstates associated with a mixing of $Q\bar{Q}$ and meson-meson configurations, we expand the wave function in terms of pure $Q\bar{Q}$ and pure meson-meson components. More precisely, we use the diabatic expansion

$$|\psi\rangle = \sum_j \int \mathrm{d}\boldsymbol{r}' \widetilde{\psi}_j(\boldsymbol{r}', \boldsymbol{r}_0) \, |\boldsymbol{r}'\rangle \, |\zeta_j(\boldsymbol{r}_0)\rangle \,, \tag{10}$$

where the light-field basis is calculated at a fixed quark-antiquark relative position $\boldsymbol{r}_0$, chosen so that string breaking effects are negligible. To make this clear, let us particularize for the case of a heavy-quark system involving $Q\bar{Q}$ and one meson-meson ($M_1\bar{M}_2$) configurations. Then we have $|\zeta_0(\boldsymbol{r}_0)\rangle \equiv |\zeta_{Q\bar{Q}}\rangle$ and $|\zeta_1(\boldsymbol{r}_0)\rangle \equiv |\zeta_{M_1\bar{M}_2}\rangle$, with the subscripts indicating the configurations associated to the light-field eigenstates, and we can relabel the diabatic wave function components as $\widetilde{\psi}_0(\boldsymbol{r}', \boldsymbol{r}_0) \equiv \psi_{Q\bar{Q}}(\boldsymbol{r}')$ and $\widetilde{\psi}_1(\boldsymbol{r}', \boldsymbol{r}_0) \equiv \psi_{M_1\bar{M}_2}(\boldsymbol{r}')$. Substituting (10), and after some straightforward manipulations, Eq. (2) can be rewritten as

$$(\mathrm{K} + \mathrm{V}(\boldsymbol{r}))\, \Psi(\boldsymbol{r}) = E\Psi(\boldsymbol{r}), \tag{11}$$

where K is the kinetic energy matrix

$$\mathrm{K} \equiv \begin{pmatrix} -\frac{\hbar^2}{2\mu_{Q\bar{Q}}}\nabla^2 & 0 \\ 0 & -\frac{\hbar^2}{2\mu_{M_1\bar{M}_2}}\nabla^2 \end{pmatrix}, \tag{12}$$

$\mu_{M_1\bar{M}_2}$ is the reduced meson-meson mass (notice that this has been easily implemented instead of $\mu_{Q\bar{Q}}$ due to the pure $M_1\bar{M}_2$ character of the corresponding wave function component), $\mathrm{V}(\boldsymbol{r})$ is the so-called *Diabatic Potential Matrix* (DPM)

$$\mathrm{V}(\boldsymbol{r}) \equiv \begin{pmatrix} V_{Q\bar{Q}}(\boldsymbol{r}) & V_{\text{mix}}(\boldsymbol{r}) \\ V_{\text{mix}}(\boldsymbol{r}) & V_{M_1\bar{M}_2}(\boldsymbol{r}), \end{pmatrix}, \tag{13}$$

with

$$V_{Q\bar{Q}}(\boldsymbol{r}) \equiv \langle \zeta_{Q\bar{Q}} | \, H^{\text{lf}}_{\text{static}}(\boldsymbol{r}) \, |\zeta_{Q\bar{Q}}\rangle \,, \tag{14a}$$

$$V_{M_1\bar{M}_2}(\boldsymbol{r}) \equiv \langle \zeta_{M_1\bar{M}_2} | \, H^{\text{lf}}_{\text{static}}(\boldsymbol{r}) \, |\zeta_{M_1\bar{M}_2}\rangle \,, \tag{14b}$$

$$V_{\text{mix}}(\boldsymbol{r}) \equiv \langle \zeta_{Q\bar{Q}} | \, H^{\text{lf}}_{\text{static}}(\boldsymbol{r}) \, |\zeta_{M_1\bar{M}_2}\rangle \,, \tag{14c}$$

and $\Psi(\boldsymbol{r})$ is a column vector notation for the wave function:

$$\Psi(\boldsymbol{r}) \equiv \begin{pmatrix} \psi_{Q\bar{Q}}(\boldsymbol{r}) \\ \psi_{M_1\bar{M}_2}(\boldsymbol{r}) \end{pmatrix}. \tag{15}$$

It can be shown that the diabatic Schrödinger equation (11) and the multichannel Schrödinger-like equation (6), particularized to the same case, are completely equivalent [18]. Here it shall suffice to mention that, as a consequence of this equivalence, the change of basis matrix A

$$\begin{pmatrix} |\zeta_{Q\bar{Q}}\rangle \\ |\zeta_{M_1\bar{M}_2}\rangle \end{pmatrix} \equiv \begin{pmatrix} |\zeta_0(\boldsymbol{r}_0)\rangle \\ |\zeta_1(\boldsymbol{r}_0)\rangle \end{pmatrix} = \mathrm{A}(\boldsymbol{r}, \boldsymbol{r}_0) \begin{pmatrix} |\zeta_0(\boldsymbol{r})\rangle \\ |\zeta_1(\boldsymbol{r})\rangle \end{pmatrix}, \tag{16}$$

transforming the diabatic wave function into the adiabatic one,

$$\psi_i(\boldsymbol{r}) = \sum_j A_{ij}(\boldsymbol{r}, \boldsymbol{r}_0)\widetilde{\psi}_j(\boldsymbol{r}, \boldsymbol{r}_0), \tag{17}$$

satisfies

$$\mathrm{A}^\dagger(\boldsymbol{r}, \boldsymbol{r}_0) \begin{pmatrix} V_0(\boldsymbol{r}) & 0 \\ 0 & V_1(\boldsymbol{r}) \end{pmatrix} \mathrm{A}(\boldsymbol{r}, \boldsymbol{r}_0) = \mathrm{V}(\boldsymbol{r}). \tag{18}$$

Equation (18) tells us that A diagonalizes the DPM, and that the eigenvalues of the DPM are nothing but $V_0(\boldsymbol{r})$ and $V_1(\boldsymbol{r})$, this is, the energies of the ground and first excited light-field states $|\zeta_0(\boldsymbol{r})\rangle$ and $|\zeta_1(\boldsymbol{r})\rangle$ calculated in unquenched Lattice QCD (see Fig. 2). So, the NACTs that break the single-channel BO approximation (Eq. (6)), when there is a significant configuration mixing, are incorporated in the diabatic approach (Eq. (11)) through the DPM.

As we show next, the DPM can be completely obtained from lattice data. This connection, together with Eqs. (3), (10), and (11), defines the diabatic approach in QCD. Specifically, from (14a) and (14b) the diagonal elements of the DPM are the static energies of light-field states associated with pure $Q\bar{Q}$ and meson-meson configurations respectively. From quenched Lattice QCD one has

$$V_{Q\bar{Q}}(\boldsymbol{r}) = V_{\mathrm{C}}(r), \tag{19}$$

where $V_{\mathrm{C}}(r)$ is a Cornell-like potential [15]. As for $V_{M_1\bar{M}_2}(\boldsymbol{r})$, one has, up to one particle exchange interactions that we neglect here,

$$V_{M_1\bar{M}_2}(\boldsymbol{r}) = T_{M_1\bar{M}_2}, \tag{20}$$

where $T_{M_1\bar{M}_2}$ is the threshold mass.

Regarding the off-diagonal element, the mixing potential $V_{\mathrm{mix}}(\boldsymbol{r})$ defined by (14c), it can be easily related to the eigenvalues $V_0(\boldsymbol{r})$ and $V_1(\boldsymbol{r})$ of the DPM, obtained as the solutions of

$$\det\left(\mathrm{V}(\boldsymbol{r}) - V_i(\boldsymbol{r})\mathrm{I}\right) = 0, \tag{21}$$

with I the identity matrix and $i = 0, 1$. Then, from (21), the radial part of the mixing is expressed as

$$|V_{\mathrm{mix}}(r)| = \frac{\sqrt{\left(V_1(r) - V_0(r)\right)^2 - \left(V_{\mathrm{C}}(r) - T_{M_1\bar{M}_2}\right)^2}}{2}. \tag{22}$$

As for the spin-angular part, it can be treated through a partial-wave analysis which is beyond the simplified notation we use here, see [23].

Hence, in the diabatic approach the $Q\bar{Q}$-$M_1\bar{M}_2$ configuration mixing problem is solved through the multichannel Schrödinger equation (11) with a potential matrix incorporating the QCD dynamics from lattice calculations.

In practical calculations, it may be convenient to interpolate the data points on $|V_{\mathrm{mix}}(r)|$, obtained by inserting lattice calculations of $V_0(r)$ and $V_1(r)$ into Eq. (22), with a continuous function. In order to yield a good fit to lattice data, this function must obviously incorporate their macroscopic features. Concretely, Eq. (22), with the energy levels of Fig. 2, seems to indicate that the mixing potential should be approximately maximum near the avoided crossing, while it should vanish away from it. A simple parametrization meeting this requirements is a Gaussian one

$$|V_{\mathrm{mix}}(r)| = \frac{\Delta}{2}\exp\left[-\frac{\left(V_{\mathrm{C}}(r) - T_{M\bar{M}}\right)^2}{2\Lambda^2}\right], \tag{23}$$

where from Eq. (22) one can see that Δ is equal to the energy gap between the ground and excited light-field energy levels at the avoided crossing, while Λ regulates the size of the region where a significant mixing between $Q\bar{Q}$ and $M_1\bar{M}_2$ takes place (see [19] for a more detailed discussion). For bottomoniumlike mesons, the values of these parameters can be obtained by fitting lattice data [16]. As for the charmoniumlike case, where lattice data is unavailable, one may fix the parameters from phenomenology, under the reasonable assumption that the same functional form may be applied.

Moreover, by expressing the radial change of basis matrix $\mathrm{A}(r)$ in terms of the $Q\bar{Q}$-$M_1\bar{M}_2$ mixing angle θ:

$$\mathrm{A}(r) \equiv \begin{pmatrix} \cos\theta(r) & -\sin\theta(r) \\ \sin\theta(r) & \cos\theta(r) \end{pmatrix} \tag{24}$$

and using (18), we have

$$\theta(r) = \frac{1}{2}\arctan\left(\frac{2V_{\mathrm{mix}}(r)}{T_{M_1\bar{M}_2} - V_{\mathrm{C}}(r)}\right). \tag{25}$$

Then, from (7) we can calculate the radial NACTs:

$$\boldsymbol{\tau}_{00}(r) = \boldsymbol{\tau}_{11}(r) = 0, \tag{26a}$$

$$\boldsymbol{\tau}_{01}(r) = -\boldsymbol{\tau}_{10}(r), \tag{26b}$$

where

$$\boldsymbol{\tau}_{01}(r) = \hat{\boldsymbol{r}}\frac{\mathrm{d}\theta}{\mathrm{d}r}. \tag{27}$$

Therefore the NACTs can be neglected only for values of r where θ is constant. From Eq. (23), one can see that this happens only for r far from the avoided crossing. There, one has θ equal to either 0 or $\pi/2$, which corresponds to a light-field eigenstate made of pure $Q\bar{Q}$ or meson-meson, respectively.

For the sake of clarity, let us emphasize that the multichannel Eq. (6) is completely equivalent to the diabatic Schrödinger Eq. (11), *if the NACTs are correctly taken into account*. Vice versa, it is trivial to show that if the NACTs vanish, then the DPM becomes a diagonal matrix containing the quenched static potentials, and therefore Eq. (11) becomes the set of single-channel Schrödinger equations (9).

The diabatic formalism can be straightforwardly generalized to the case of N meson-meson thresholds through a kinetic energy matrix (null matrix elements are omitted)

$$\mathrm{K} = \begin{pmatrix} -\frac{\hbar^2}{2\mu_{Q\bar{Q}}}\nabla^2 & & & \\ & -\frac{\hbar^2}{2\mu^{(1)}_{M\bar{M}}}\nabla^2 & & \\ & & \ddots & \\ & & & -\frac{\hbar^2}{2\mu^{(N)}_{M\bar{M}}}\nabla^2 \end{pmatrix}, \tag{28}$$

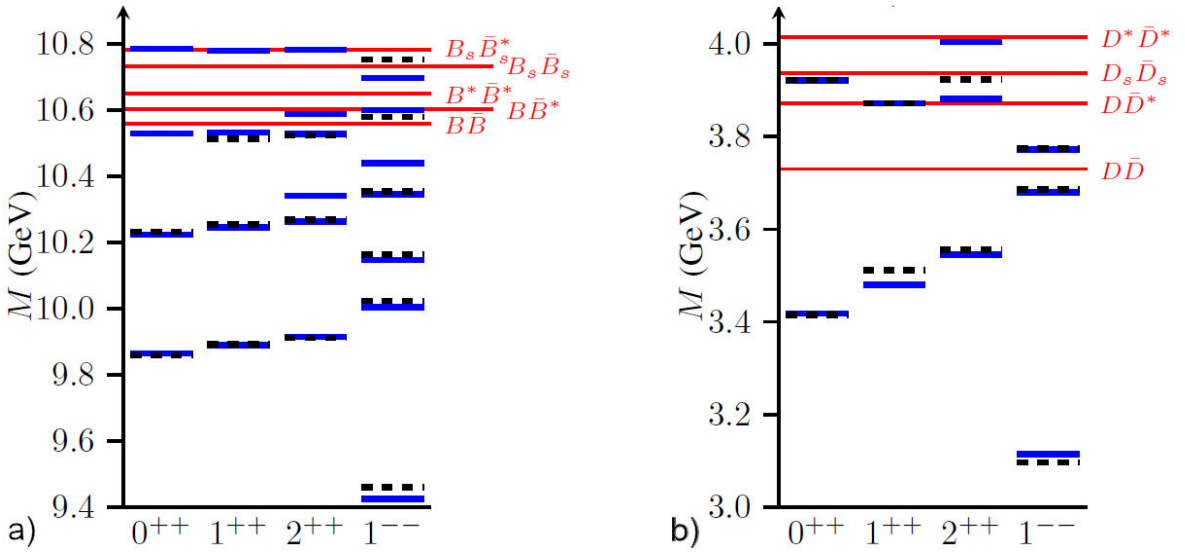

FIGURE 3. Spectrum of bottomoniumlike (left) and charmoniumlike (right) meson states. Thick solid lines stand for states calculated in the diabatic approach, thick dashed lines stand for well-established experimental candidates, and long thin horizontal lines stand for open-flavor meson-meson thresholds.

where $\mu^{(i)}_{M\bar{M}}$ with $i = 1, \ldots, N$ is the ith meson-meson component reduced mass, and a generalized DPM containing the interaction. For the sake of simplicity, and in line with Lattice QCD studies of string breaking [17], one usually neglects some interactions between channels. Specifically, one may assume, as long as we are dealing with relatively narrow, well-separated thresholds, that interactions between different meson-meson components are negligible. Then, the DPM can be written as

$$\mathrm{V}(\boldsymbol{r}) = \begin{pmatrix} V_{\mathrm{C}}(r) & V^{(1)}_{\mathrm{mix}}(\boldsymbol{r}) & \cdots & V^{(N)}_{\mathrm{mix}}(\boldsymbol{r}) \\ V^{(1)}_{\mathrm{mix}}(\boldsymbol{r}) & T^{(1)}_{M\bar{M}} & & \\ \vdots & & \ddots & \\ V^{(N)}_{\mathrm{mix}}(\boldsymbol{r}) & & & T^{(N)}_{M\bar{M}} \end{pmatrix}, \quad (29)$$

where $V_{\mathrm{C}}(r)$ is the Cornell potential, $T^{(i)}_{M\bar{M}}$ the mass of the ith threshold and $V^{(i)}_{\mathrm{mix}}(\boldsymbol{r})$ the mixing potential between the $Q\bar{Q}$ and the ith meson-meson components.

For practical calculations, one should also realize that a meson-meson component does not intervene in the composition of a bound state with a mass far below its threshold. Hence, finding the spectrum of some J^{PC} heavy-quark meson family consists in solving a multichannel Schrödinger equation involving only the $Q\bar{Q}$ and those "close" meson-meson channels coupling with the specific J^{PC} quantum numbers.

4. Results

The diabatic framework can be an effective tool for a unified study of the quarkoniumlike meson spectrum, since it treats the $Q\bar{Q}$ interaction, responsible for the spectrum of conventional quarkonium states, on equal grounds with the $Q\bar{Q}$–meson-meson mixing one, responsible for the appearance of some unconventional states and the OZI-allowed decays of states above an open-flavor meson-meson threshold. To show this more clearly, we recollect here the results of a diabatic study of the bottomoniumlike [21] and charmoniumlike [19, 20] spectra. Let us note that the parameters used in the diabatic potential matrix are obtained from a mixture of lattice data and phenomenology. More precisely, the parameters of the Cornell-like potential $V_{\mathrm{C}}(r)$ are taken from phenomenology, the threshold masses are obtained from the sum of the corresponding experimental meson masses [5], and the parameters of the mixing potential are inferred from lattice calculations in the bottomoniumlike case [21], or fitted using the mass of $X(3872)$ in the charmoniumlike case [19].

The calculated spectra of bottomoniumlike and charmoniumlike mesons are illustrated in Fig. 3, and the OZI-allowed strong decay widths of states above threshold are reported in Tables I and II. From these results we see that the diabatic quarkoniumlike meson spectrum is composed of conventional quarkonium states plus a certain number of unconventional ones lying close to some open-flavor meson-

TABLE I. Calculated masses and OZI-allowed strong decay widths of bottomoniumlike states above threshold, in MeV.

J^{PC}	M	$\Gamma_{B\bar{B}}$	$\Gamma_{B\bar{B}^*}$	$\Gamma_{B^*\bar{B}^*}$	$\Gamma_{B_s\bar{B}_s}$	$\Gamma^{\mathrm{Theor}}_{\mathrm{total}}$
0^{++}	10785.8	1.6		5.3	0.7	7.6
1^{++}	10778.9		0.2	1.7		1.9
2^{++}	10588.4	4.3				4.3
2^{++}	10782.3	5.4	1.5	21.0	10.4	38.3
1^{--}	10599.8	21.9				21.9
1^{--}	10697.0	2.0	1.0	38.0		41.0

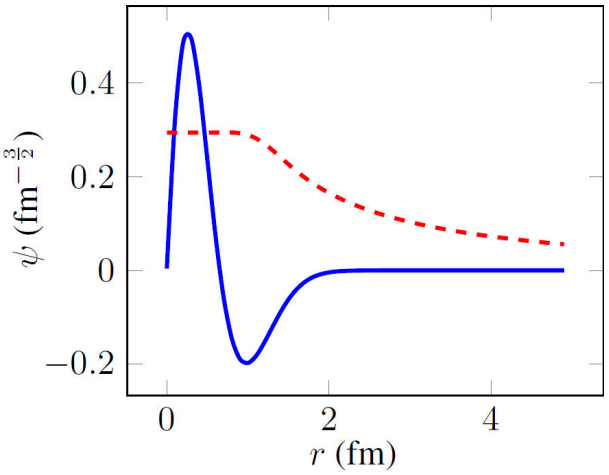

FIGURE 4. Diabatic radial wave function of $X(3872)$. Solid and dashed line stand for the $c\bar{c}$ and $D\bar{D}^*$ component, respectively.

TABLE II. Calculated masses and OZI-allowed strong decay widths of charmoniumlike states above threshold, in MeV.

J^{PC}	M	$\Gamma_{D\bar{D}}$	$\Gamma_{D\bar{D}^*}$	$\Gamma_{D_s\bar{D}_s}$	$\Gamma^{\text{Theor}}_{\text{total}}$
0^{++}	3920.9	0.6			0.6
2^{++}	3881.1	49.5	0.4		49.9
2^{++}	4003.9	4.8	6.3	3.5	14.5
1^{--}	3771.7	20.2			20.2

meson threshold. As for the calculated widths of states above threshold, they can be compared with those of the few well-established experimental candidates. So in the bottomoniumlike case, the $\Upsilon(4S)$ with a total experimental width of 20.5 ± 2.5 MeV is perfectly compatible, within errors, with the diabatic 1^- state at around 10.6 GeV with a total calculated width of 21.9 MeV. In the charmoniumlike case, on the other hand, there are two experimental candidates, the $\psi(3770)$ and the $\chi_{c2}(3930)$, respectively for the 1^- diabatic state near 3.77 GeV and the 2^{++} one around 3.88 GeV. The calculated widths are in this case fairly close (only about 30% off) the experimental values of 27.2 ± 1.0 MeV for $\psi(3770)$ and 35.2 ± 2.2 MeV for $\chi_{c2}(3930)$. The overall reasonable description of both the spectrum and decay widths gives further support to the mixing potential being the main mechanism driving the appearance of unconventional quarkonium-like states as well as the OZI-allowed decay of states above threshold.

It is particularly interesting to detail the diabatic description of $X(3872)$ obtained from this study. As can be checked in Fig. 4, the diabatic $X(3872)$ is made, at short distances, of both $c\bar{c}$ and $D\bar{D}^*$ components in comparable amounts. But then, for bigger distances, the confined $c\bar{c}$ component vanishes more quickly than the loosely bound $D\bar{D}^*$ one, so that the molecular configuration dominates the overall composition of $X(3872)$ (97% total $D\bar{D}^*$ probability vs. 3% $c\bar{c}$). This makes the $X(3872)$ mostly a $D\bar{D}^*$ molecule, with a calculated mean root-mean-square radius of near 11 fm, where the binding is provided by the $D\bar{D}^*$ mixing with the confined $c\bar{c}$ component.

5. Summary

The diabatic formalism can be used to describe heavy-quark mesons beyond the limitations of the single-channel approximation commonly used in BO. This allows for a general treatment of quarkoniumlike meson states, including those for which mixing between quark-antiquark and meson-meson configurations plays a significant role. The diabatic dynamics, directly connected to lattice data, can give account of the mass spectrum and OZI-decay widths of heavy-quark mesons, as shown through a calculation of the bottomoniumlike and charmoniumlike meson spectra and properties. This makes the diabatic approach in QCD a useful theoretical framework for the unified description of conventional quarkonium and unconventional quarkoniumlike meson states.

This work has been supported by Ministerio de Ciencia e Innovación and Agencia Estatal de Investigación of Spain and European Regional Development Fund Grant No. PID2019-105439 GB-C21, by EU Horizon 2020 Grant No. 824093 (STRONG-2020), and by Conselleria de Innovación, Universidades, Ciencia y Sociedad Digital, Generalitat Valenciana GVA PROMETEO/2021/083. R. B. acknowledges a FPI fellowship from Ministerio de Ciencia, Innovación y Universidades of Spain under Grant No. BES-2017-079860.

1. S.-K. Choi *et al.* (Belle Collaboration), Observation of a Narrow Charmoniumlike State in Exclusive $B^{\pm} \to K^{\pm}\pi^{+}\pi^{-}J/\psi$ Decays, *Phys. Rev. Lett.* **91** (2003) 262001, https://dx.doi.org/10.1103/PhysRevLett.91.262001.

2. E. J. Eichten, K. Gottfried, T. Kinoshita, K. D. Lane, and T. M. Yan, Charmonium: The model, *Phys. Rev. D* **17** (1978) 3090, https://dx.doi.org/10.1103/PhysRevD.17.3090.

3. E. J. Eichten, K. D. Lane, and C. Quigg, Charmonium levels near threshold and the narrow state $X(3872) \to \pi^{+}\pi^{-}J/\psi$, *Phys. Rev. D* **69** (2004) 094019, https://dx.doi.org/10.1103/PhysRevD.69.094019.

4. S. Godfrey and N. Isgur, Mesons in a relativized quark model with chromodynamics, *Phys. Rev. D* **32** (1985) 189, https://dx.doi.org/10.1103/PhysRevD.32.189.

5. P. A. Zyla *et al.* (Particle Data Group), Review of particle physics, *Progr. Theor. Exp. Phys.* **2020** (2020) 083C01, https://dx.doi.org/10.1093/ptep/ptaa104.

6. T. Barnes and E. S. Swanson, Hadron loops: General theorems and application to charmonium, *Phys. Rev. C* **77** (2008)

055206, https://dx.doi.org/10.1103/PhysRevC.77.055206.

7. J. Ferretti and E. Santopinto, Threshold corrections of $\chi_c(2P)$ and $\chi_b(3P)$ states and $J/\psi\rho$ and $J/\psi\omega$ transitions of $X(3872)$ in a coupled-channel model, *Phys. Lett. B* **789** (2019) 550, https://dx.doi.org/10.1016/j.physletb.2018.12.052.

8. H.-X. Chen, W. Chen, X. Liu, and S.-L. Zhu, The hidden-charm pentaquark and tetraquark states, *Phys. Rep.* **639** (2019) 1, https://dx.doi.org/10.1016/j.physrep.2016.05.004.

9. R. F. Lebed, R. E. Mitchell, and E. S. Swanson, Heavy-quark QCD exotica, *Prog. Part. Nucl. Phys.* **93** (2017) 143, https://dx.doi.org/10.1016/j.ppnp.2016.11.003.

10. F.-K. Guo *et al*., Hadronic molecules, *Rev. Mod. Phys.* **90** (2018) 015004, https://dx.doi.org/10.1103/RevModPhys.90.015004.

11. A. Esposito, A. Pilloni, and A. Polosa, Multiquark resonances, *Phys. Rep.* **668** (2017) 1, https://dx.doi.org/10.1016/j.physrep.2016.11.002.

12. K. J. Juge, J. Kuti, and C. J. Morningstar, Ab Initio Study of Hybrid $\bar{b}gb$ Mesons, *Phys. Rev. Lett.* **82** (1999) 4400, https://dx.doi.org/10.1103/PhysRevLett.82.4400.

13. E. Braaten, C. Langmack, and D. H. Smith, Born-Oppenheimer approximation for the XYZ mesons, *Phys. Rev. D* **90** (2014) 014044, https://dx.doi.org/10.1103/PhysRevD.90.014044.

14. N. Brambilla *et al*., The XYZ states: experimental and theoretical status and perspectives, *Phys. Rep.* **873** (2020) 1, https://dx.doi.org/10.1016/j.physrep.2020.05.001.

15. G. S. Bali, QCD forces and heavy quark bound states, *Phys. Rep.* **343** (2001) 1, https://dx.doi.org/10.1016/S0370-1573(00)00079-X.

16. G. S. Bali, H. Neff, T. Düssel, T. Lippert, and K. Schilling (SESAM Collaboration), Observation of string breaking in QCD, *Phys. Rev. D* **71** (2005) 114513, https://dx.doi.org/10.1103/PhysRevD.71.114513.

17. J. Bulava *et al*., String breaking by light and strange quarks in QCD, *Phys. Lett. B* **793** (2019) 493, https://dx.doi.org/10.1016/j.physletb.2019.05.018.

18. M. Baer, *Beyond Born-Oppenheimer: Electronic Nonadiabatic Coupling Terms and Conical Intersections* (John Wiley & Sons, New York, 2006).

19. R. Bruschini and P. González, Diabatic description of charmoniumlike mesons, *Phys. Rev. D* **102** (2020) 074002, https://dx.doi.org/10.1103/PhysRevD.102.074002.

20. R. Bruschini and P. González, Diabatic description of charmoniumlike mesons. II. Mass corrections and strong decay widths, *Phys. Rev. D* **103** (2021) 074009, https://dx.doi.org/10.1103/PhysRevD.103.074009.

21. R. Bruschini and P. González, Diabatic description of bottomoniumlike mesons, *Phys. Rev. D* **103** (2021) 114016, https://dx.doi.org/10.1103/PhysRevD.103.114016.

22. M. Born and R. Oppenheimer, ForeignlanguagegermanZur quantentheorie der molekeln, *Ann. Phys.* **389** (1927) 457, https://dx.doi.org/10.1002/andp.19273892002.

23. R. Bruschini and P. González, Coupled-channel meson-meson scattering in the diabatic framework, *Phys. Rev D* **104** (2021) 074025, https://dx.doi.org/10.1103/PhysRevD.104.074025.